EXPERIMENTAL AND MECHANISTIC INVESTIGATION OF OPPOSED-FLOW PROPANE/AIR FLAMES BY PHOSPHORUS-CONTAINING COMPOUNDS

by

Richard T. Wainner, Kevin L. McNesby,
Robert G. Daniel, and Andrzej W. Miziolek
US Army Research Laboratory
and
Valeri I. Babushok
Building and Fire Research Laboratory
National Institute of Standards and Technology
Gaithersburg, MD 20899 USA

Reprinted from the Halon Options Technical Working Conference. Proceedings. HOTWC 2000. Sponsored by: University of New Mexico, Fire Suppression Systems Assoc., Fire and Safety Group, Great Lakes Chemical Corp., Halon Alternative Research Corp., Hughes Associates, Inc., Kidde Fenwal, Inc., Kidde International, Modular Protection, Inc., Next Generation Fire Suppression Technology Program, Sandia National Laboratories, Summit Environmental Corp., Inc. and 3M Specialty Materials. May 2-4, 2000, Albuquerque, NM, 2000.

NOTE: **This paper is a contribution of the National Institute of Standards and Technology and is not subject to copyright.**

NIST CENTENNIAL 1901-2001

NIST

National Institute of Standards and Technology
Technology Administration, U.S. Department of Commerce

EXPERIMENTAL AND MECHANISTIC INVESTIGATION OF OPPOSED-FLOW PROPANE / AIR FLAMES BY PHOSPHORUS-CONTAINING COMPOUNDS

Richard T. Wainner, Kevin L. McNesby,
Robert G. Daniel, and Andrzej W. Miziolek
US Army Research Laboratory

Valeri I. Babushok
National Institute of Standards & Technology

ABSTRACT

In this work, we report the results of experimental and computational studies on inhibition and extinction of opposed-flow propane (C_3H_8)-air flames by DMMP ($C_3H_9O_3P$), as well as N_2 and FM-200 (C_3F_7H) as reference inhibitors. For the dilute flame conditions used in this work (high Z_{st}), inhibitor effectiveness was significantly enhanced compared to previous results with undiluted fuel. However, unlike the previous work, OH fluorescence signals, and thus concentrations, did not decrease as the inhibitant concentration was increased, even near extinction. The cause for this remains to be determined. Modeling results for a 1-D opposed flow flame of the same conditions agree with the present results of steady OH levels, while having also predicted the decreasing levels for the previous work with undiluted fuel.

INTRODUCTION

Data in the literature show a large number of phosphorus-containing compounds (PCC) to be very effective fire suppressants. A number of investigations were performed on liquid PCCs in premixed and diffusion flames in the 1960s [1-6]. Since that time, a large amount literature on the use of solid PCCs as flame inhibitors has been amassed [7], while a number of compounds have seen use as fire retardants in materials and in dry chemical fire extinguishers [8]. The references to phosphorus-containing liquids or gases as flame suppressants are few [9-16]. On a molar basis, PCCs have been shown to be more than 40 times more effective than N_2 and 2–4 times more effective than CF_3Br. Typically, the range of extinction concentrations is 0.5–5.0 vol%.

A fast-acting, effective fire suppressant is what is required to meet the Army's demand for the detection and extinguishment of a fuel fireball in the crew compartment of an armored vehicle in less than 250 ms. A demand exists for a safe fire inhibitor of this capability not only for the logic of using the most effective compound available, but also because one of the most widely used chemically acting suppressants, Halon 1301 (CF_3Br), has been banned from production since 1992 due to its stratospheric ozone-depleting capability [17]. Halogens and phosphorus can also be blended, with a mixture of species or in the same molecule. Some research has been performed on the effectiveness of halogenated PCCs [6, 11, 15]. However, on a per weight basis, these performed no better than the unhalogenated PCCs [11]. Also, halogenated compounds tend to produce toxic products from combustion. It has been postulated that phosphorus-containing radical species catalyze the recombination of H and OH in the combustion zone and some evidence exists of H and OH being affected by PCC addition [6, 13, 16, 18, 19]. Some data show the effectiveness of PCCs to decrease with higher flame temperatures [10, 13]. It has also been suggested that only the presence and availability of the P atom itself is the sole determiner of the concentration of species such as HPO_2, $HOPO_2$, and HOPO, and is thus the dominant requirement for flame inhibition [7, 14, 19]. However, some evidence indicates that aromatic phosphorus ring compounds may not be as effective for flame inhibition [13, 14]. Particular attention is thus called to the different behavior of P-N ring compounds and P-O compounds. One explanation might be that phosphorus atoms are more bound in these compounds.

Several different methods exist for measuring the effectiveness of a potential flame inhibitor. The air side extinction concentration for diffusion flames generated by a cup burner is a long-standing gauge [20]. Other measures exist in the form of flame speeds for premixed flames, flame heat release, global oxidizer-side strain rate at extinction for diffusion flames, and radical species concentrations. This work will measure inhibitor concentrations at extinction and will employ planar laser-induced fluorescence (PLIF) for imaging the concentration of the OH radical through the flame. The determination of the inhibiting effectiveness of various PCCs and the effect of molecular structure is one goal of this research. Another goal is the development and validation of an accurate chemical mechanism for the prediction of phosphorus chemistry in a combustion environment. While the end objective of this research will be to look at a number of phosphorus compounds experimentally and computationally, including DMMP, $P_3N_3F_6$, and $P_3N_3(CH_3O)_6$, this report summarizes the current results obtained with DMMP in comparison to N_2 and FM-200, as well as a comparison to model results with the current developed phosphorus chemistry mechanism.

PHOSPHORUS CHEMISTRY

The kinetic model of flame inhibition by PCCs (Appendix A) is based on the kinetic data used for the analysis of the influence of PH3 combustion products on the radical recombination rates in a hydrogen flame and on kinetic models used for describing destruction of DMMP and TMP in a low pressure hydrogen flame [18, 19, 21].* (Estimates were also used from selected references [19, 21, 22]). Reactions of phosphorus-containing species with radicals and intermediate species of hydrocarbon combustion have been included. Reactions have been added to the scheme to complete the reaction pathways for the consumption of some of the species. The data have been adjusted to take into account recent thermochemical and kinetic data for phosphorus-containing species. Figure 1 shows an abbreviated map of the DMMP decomposition and inhibition reactions. Following decomposition, the main phosphorus -containing species in the flame are PO_2, HOPO, and $HOPO_2$. Numerical calculations for a premixed flame [7] and a sensitivity analysis show that the burning velocity is most sensitive to the rate of two recombination reactions: (1) $H + PO_2 + M \Leftrightarrow HOPO + M$ (2) $OH + PO_2 + M \Leftrightarrow HOPO_2 + M$. One important characteristic of the model is that the inhibition properties of the PCC are determined by the phosphorus molecule content [7, 19].

EXPERIMENTAL METHODS

DIFFUSION FLAME

Measurements were made in a sizeable, axisymmetric, counterflow diffusion flame. The nominally flat flame is produced by vertically aligned opposing jets of oxidizer and fuel. The burner head gas outlets are designed for essentially uniform and parallel flow. Gases are directed through a series of mesh and porous steel plates, with one of these porous plates serving as the final gas outlet. These ducts are 7.0 cm in diameter and are separated by a distance of 2.5 cm.

* Mokrushin, V., Bolshova, T., Korobeinichev, O. P., "A Kinetic Model for the Destruction of TMP in a Hydrogen/Oxygen Flame," unpublished, 1998.

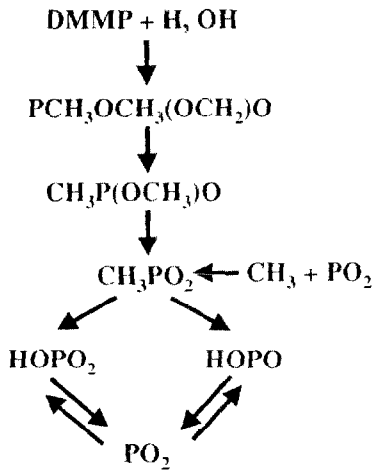

Figure 1. Abbreviated DMMP decomposition and inhibition cycle. Most pathways are sustained by the chain carrying radical species H, O, and OH.

The heads themselves are enclosed in a large airtight steel chamber connected to an exhaust manifold and then to a vacuum pump. Four short arms protrude off the chamber with two exits to the exhaust manifold in each. These arms terminate in plates with windows mounted to them, providing optical access to the flame for diagnostics and visualization. A nitrogen purge is provided to the inside surface of the windows to prevent condensation and soot buildup. Each burner head can be translated in two directions and moved in unison, allowing optical and physical probes to investigate different regions of the flame while the probes remain fixed. Cooling water is provided to coils around the burner heads and around the outside of the burner chamber.

The flow conditions for the nominally "neat" flame are 40.0 L/min of air from the upper (oxidizer) duct and 36.0 L/min nitrogen (N_2) plus 3.4 L/min propane (C_3H_8) from the lower (fuel) duct (~17 cm/s velocities). The vacuum pump holds the combustion chamber at moderate negative pressure (650 ± 10 Torr) to evacuate the combustion products. The gas flows are metered by mass-flow controllers and calibrated with a wet test flow meter. These flowrates provide a set of opposed jets that are close to momentum-balanced ($r_O V_O^2 = r_F V_F^2$), yielding a stagnation plane for the colliding flows that sits at the center of the burner gap. When ignited, this provides a non-sooting, blue flame that sits just barely on the oxidizer side of the stagnation plane. While significantly different from a fuel fireball scenario, this dilute, and thus relatively cool, flame provides several advantages. Additive concentrations reaching the flame zone from the fuel side will be close to those achieved by oxidizer-side addition. There is no soot to interfere with optical measurements in situ, along the optical path, or on the windows. Secondly, previous work has shown some PCCs to be more effective flame suppressors (per mole inhibitor) at higher dilutions, and thus lower flame temperatures [9, 10]. Last, as a result, significant expense is avoided by using less inhibitor, as even very small vol% concentrations translate to significant masses at these flowrates.

INHIBITOR ADDITION

Additives to the neat conditions are introduced on the oxidizer side only. This is representative of a real world extinguisher delivery system. However, while N_2 and FM-200 can be delivered easily in gaseous form (FM-200 has ~50 psig vapor pressure), the vapor pressure of DMMP at room temperature is not large (<1 Torr). Therefore, DMMP addition to the airstream was per-

formed as illustrated in Figure 2. An injection pump capable of metering between 0.001 and 2000 μl/min delivered preheated DMMP into the preheated air stream. The injected DMMP vaporizes and mixes with the incoming air. Heating tape (with thermocouple feedback control) held the additive, incoming air, and mixture lines at 80 °C all the way to the burner.

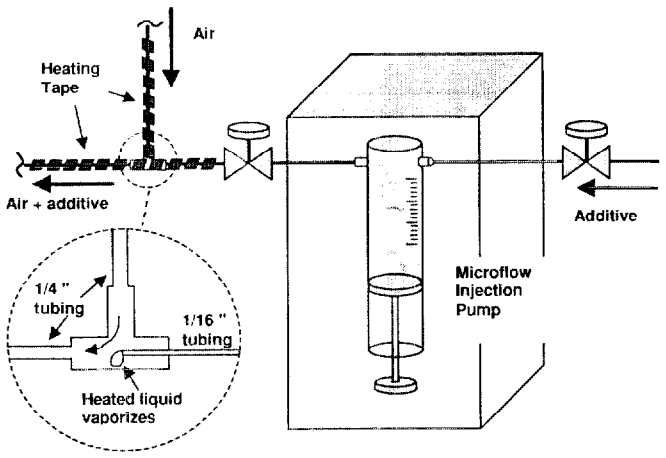

Figure 2. Schematic of setup for introducing and metering liquid inhibitors of low vapor pressure. For the DMMP additions of this work, air and additive lines beyond the injection pump exit valve are held at 80 °C.

OH LIF

OH concentrations in the flame zone were monitored with varying inhibitor concentrations up to flame extinction via planar laser-induced fluorescence (PLIF) imaging. The observed PLIF signals were generated by the frequency-doubled output of a narrow-linewidth dye laser, which was pumped by a XeCl excimer laser (Lambda Physik models SCANmate 2 and COMPex 102, respectively). The pump laser, and thus output beam, were run at 10 Hz. Coumarin 153 dye was employed to produce output wavelengths near 565 nm (doubled output near 282.5 nm). The tuning resolution of the dye laser is 0.001 nm. For OH imaging, the UV beam was tuned to an absorbing transition in the (1,0) band of the $A^2\Sigma^+ \rightarrow X^2\Pi$ electronic transition, specifically the Q_1 branch (J"=4.5) at 282.439 nm. The wavelength tuning was computer controlled and monitored. Several excitation wavelength scans were performed to ascertain the exact delivered wavelength by comparing to a simulated excitation scan from published transition data [23]. The computer/motor control had some offset error (~.025 nm) and some hysteresis. Hysteresis was monitored by imaging a small fraction of the beam (picked off with a microscope slide) through an air-spaced etalon, changing the beam into an Airy ring system, and into a monochromator with imaging detector. This also showed the spectral width of the beam to be 0.0085 nm FWHM. The laser energy varied from 1.25 to 0.85 mJ, due to dye degradation.

The output beam (~1 mm dia.) is directed into the center of the burner gap through an aperture and spread vertically into a sheet with a cylindrical lens (70 mm f.l.) (Figure 3). The beam was sufficiently spread that the entire distance between the burner heads (~1 mm wide sheet) was illuminated and that the intensity across the reaction (OH-containing) zone was essentially uniform. Laser power was monitored between times of data recording with a volumetrically absorbing power meter. Shot-to-shot intensities were stable to within 7%.

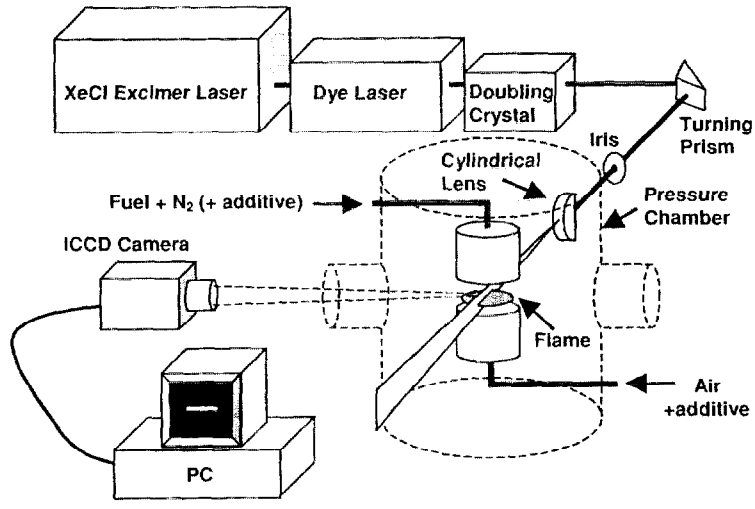

Figure 3. Laser-induced fluorescence experimental setup. Flow conditions for "neat" flame are 40 L/min air (upper head) and 36 L/min N_2 + 3.4 L/min C_3H_8 (lower head). Combustion chamber pressure is typically at 650 Torr. Laser excitation is at 282.438 nm. Optical filtering may also be applied to light reaching the camera.

OH fluorescence signals were recorded with an intensified CCD camera (Princeton Instruments ITE-CCD) as close as possible to the window at a right angle to the laser beam. Fluorescence emission was recorded broadband, over the full temporal and spectral region of OH LIF. The full burner gap was imaged and most of the width (Figure 4). Pixel resolution is 83 μm. Images are 100-shot accumulations. Some background signal level existed from scattering and dark counts. These contributions were subtracted from the acquired images and day-to-day signals were normalized by the laser energy. The laser energies used in all of these measurements were within the range of linear response of OH signal to laser energy. OH concentration profiles across the flame were obtained by integrating signals along a 0.5 cm (60 pixel) width near the center of the flame, at a relatively flat portion of the flame, as represented by the rectangle superimposed on the image of Figure 4. Overall OH signal levels for each measured set of flame conditions are achieved by integrating over the 2-D profile just described, resulting in a single data point. Only relative signals are reported in this work. Future measurements will entail a calibration with a line-of-sight OH absorption measurement.

NUMERICAL MODELING

The phosphorus kinetic model under development was tested in two separate efforts. First, the model was included in a previously developed kinetic model for the combustion of C_1 to C_4 hydrocarbons and run in a commercially available 1-D opposed-flow flame code, namely OPPDIF [24]. The conditions in this simulation were defined to match the experiments of this work. Secondly, the model was run for the methane-air flame conditions of MacDonald et al. [9, 10] for both plug flow and potential flow boundary conditions using the procedure developed by Nishioka et al. [25].

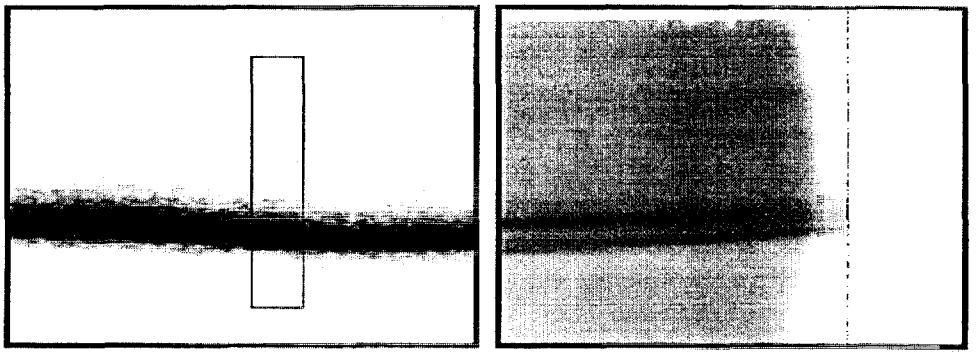

Figure 4. Left: Sample 100-shot OH fluorescence image for "neat" conditions. Right: Flame luminescence. (Window opposite camera is uncovered. Light streak is an air tube outside the window. Nonuniformities in the flows can be seen in the slight wrinkling of the flame. This develops as portions of the porous plate become somewhat clogged.) Signal intensities for both images are inversely scaled from light to dark. Scattered laser light from the lower burner head can be seen at the bottom of the left image. Rectangle represents region of horizontal integration for extracting OH profiles.

RESULTS

The first experiment performed entailed an effort to visualize the stagnation plane and mixing zone. This was achieved by introducing acetone vapor into each gas stream, successively. Acetone fluorescence was induced by a laser sheet directly from the excimer laser (308 nm, 210 mJ). Figure 5 is a processed image resulting from the multiplication of images acquired with fuel side and air side addition. The stagnation plane and region of significant diffusion (mixing region) are apparent. These flows were nonreacting.

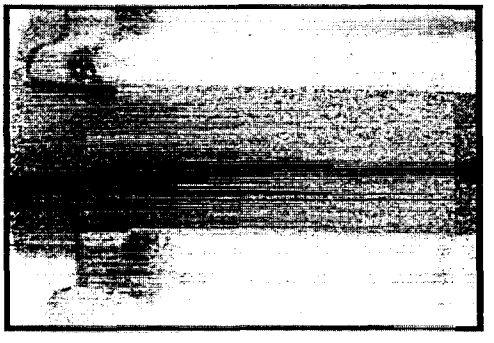

Figure 5. Image resultant from the product of images of acetone fluorescence with fuel- and air-side seeding.

Figure 6 compares model results with experimental data for the given flame inhibited by DMMP. Figure 6a is a comparison of OH concentration profiles for the "neat" conditions. The experimental data have been normalized to the peak level of the model data. While the experimental distribution is slightly wider than the model result, the agreement is relatively good. Contrary to expectations, however, no decrease in OH signal level was observed for increasing amounts of DMMP delivered to the flame. Figure 6b shows that within measurement error, the signals were

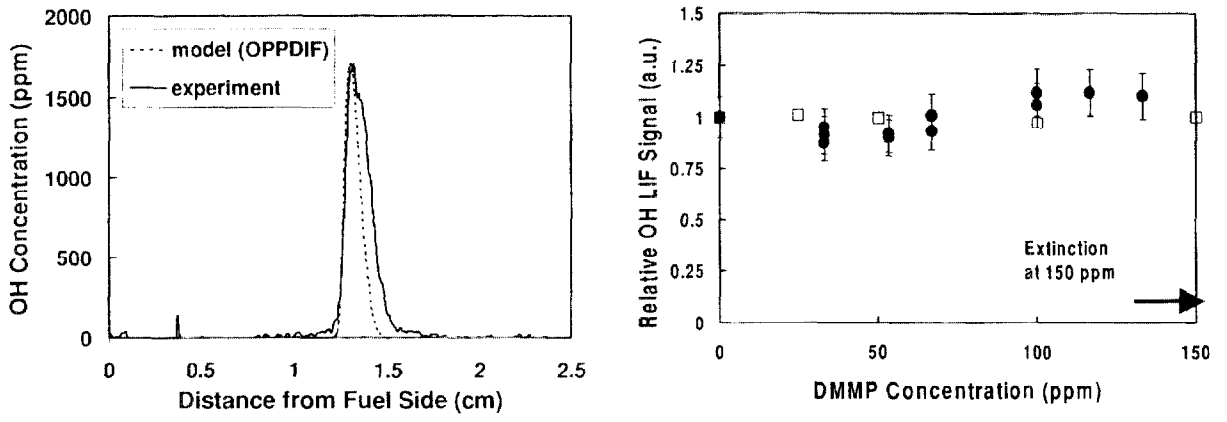

(6a) (6b)

Figure 6. OH concentrations. (6a): Model result for OH concentration through the flame compared to experimental OH LIF signals for the "neat" flow conditions. Data are normalized at the peak. (6b): Integrated OH LIF signals (experiment) and concentrations (model) versus amount of DMMP added to the flame.

relatively flat. Interestingly, the model results agree with this lack of response. The reason for the behavior of each is unknown at this time.

The above results support the accuracy of the model. Also, the numerical simulation indicates that while OH levels hold steady, phosphorus-containing radicals do increase with added DMMP. The compound does seem to act in a chemical manner. The flame is put out with only 150 ppm DMMP. This is not because the flame is right on the edge of thermal stability. A much greater amount (8%) of N_2 (physically acting molecule) is required to suppress the flame. Measurements were also performed for FM-200, indicating an extinction concentration of 525 ppm. FM-200 inhibition also did not reveal any changes in OH levels. The relative effectiveness of the two chemically acting compounds is much closer than in previous work with the undiluted flame (0.3 and 5.3%). An effort was made to run a less diluted flame for comparison to previous work, but soot in the burner chamber and on the windows became a problem for propane concentrations greater than 20%. Initial measurements with $P_3N_3(CH_3O)_6$ were also made, but due to a low vapor pressure, additive seeding and metering is a challenge. The initial attempt shows that the extinction concentration is greater than 100 ppm. Table 1 displays the relative extinction concentrations for the current and previous work, normalized to the N_2 data.

TABLE 1. RELATIVE EXTINCTION CONCENTRATIONS FOR VARIOUS PCCS. DATA ARE NORMALIZED TO THE RESULTS FOR N_2.

	Relative Extinction Concentrations				
	N_2	FM-200	DMMP	PN Meth	Hexa-F PN
This Work	1.0 ± 0.056	0.0065 ± 0.00019	0.00019 ± 0.00013	> 0.0013	
Previous Work	1.0 ± 0.35	0.23 ± 0.043	0.0130 ± 0.0017		0.117 ± 0.043

As mentioned, numerical simulations were also conducted for the PCC-inhibited flames of other current research [9, 10]. The aim was to obtain the dependence of the extinction strain rate as a function of inhibitor concentration for plug- and potential-flow boundary conditions and to compare with experimental data. These experiments [9, 10] showed that the addition 0.15% DMMP reduces the extinction strain rate by 35%. Calculations with the suggested kinetic model and the same conditions indicate a decrease in the extinction strain rate of approximately 30% for the same concentration of DMMP. Figure 7 displays the dependency of the normalized global strain rate on flame temperature for an inhibited and uninhibited flame. An increase in DMMP concentration leads to a decrease in the global strain rate. The turning point of the curve corresponds to the extinction conditions.

Calculated extinction concentrations for flow rates of 30cm/s are the following: 2.2% (molar percentage, plug-flow boundary conditions) and 3.6 (potential-flow boundary conditions) (Figure 7). The calculated suppression concentration for premixed flames is in the range 2.8-3.2% using critical burning velocity criteria and represents an intermediate value. Calculations of DMMP and CF_3Br inhibited flames also demonstrate that an increase in inhibitor concentration leads to a shift of the OH concentration profile away from the oxidizer side and to a decrease of flame thickness. This was observed in previous experiments along with a downward trend of OH concentration with increasing inhibitor [16].

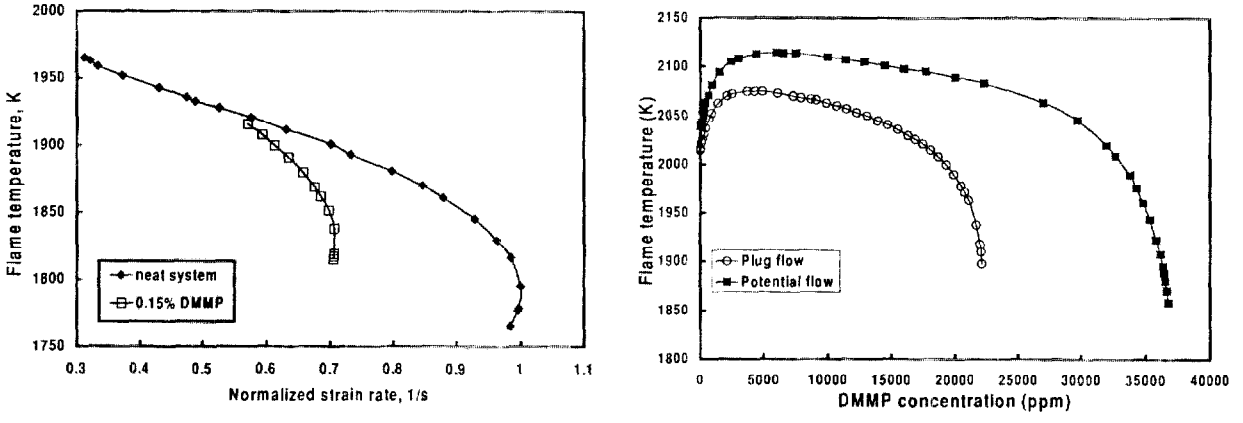

(7a) (7b)

Figure 7. (7a): Dependence of a maximum flame temperature (inhibited and unihibited) on the normalized global strain rate. Methane/Air flame conditions as in Refs. 9 and 10. Burner gap is 0.95 cm. (7b): Flame temperature dependence on DMMP addition for plug- and potential-flow boundary conditions (30 cm/s flows).

CONCLUSIONS

Chemical inhibition experiments were performed in a near atmospheric pressure, low strain, dilute opposed-flow flame. These conditions proved to be very sensitive to the addition of inhibitive agents. For DMMP, 150 ppm was sufficient to extinguish the flame. Though the flame is cool, the strong inhibition effectiveness should not be due to being near the physical (thermal) extinction limit, as a full 8% N_2 addition is required to extinguish the flame. The increased effectiveness of the chemical inhibitors relative to N_2 compared to the undiluted flame work is of much interest.

While the flame seems more sensitive to chemical inhibition, the concentration of the radical species OH shows no signs of being affected by the concentration of inhibitor, right up to the point of extinction. Broadband, planar, laser-induced fluorescence emissions from OH are essentially constant as inhibitor concentration is varied. An explanation for this behavior is not apparent. However, a numerical model of the same conditions with a newly developed model for phosphorus chemistry show the same OH insensitivity to DMMP concentration.

Calculations of extinction concentrations were performed for opposed flow diffusion flames with different boundary conditions. Extinction concentrations (flow rate 30cm/s) are the following: 2.2% (molar percentage, plug-flow boundary conditions) and 3.6% (potential-flow boundary conditions). The calculated extinction concentration for a premixed flame represents an intermediate value (2.8-3.2%). The modeling of extinction strain rates corresponds to the experimental data of MacDonald et al. [9, 10].

ACKNOWLEDGMENTS

This work is supported by the Next-Generation Fire Suppression Technology Program (NGP) and the American Society for Engineering Education (ASEE).

REFERENCES

1. Lask, G., and Wagner, H.G., "Influence of Additives on the Velocity of Laminar Flames," *Proc. of the 8th Symp. (International) on Combust.*, pp. 432-438, 1960.
2. Rosser, W.A., Jr., Inami, S.H., and Wise, H., "The Quenching of Premixed Flames by Volatile Inhibitors," *Combustion and Flame*, 10, No. 3, pp. 287-294, 1966.
3. Miller, D.R., Evers, D.L., and Skinner, G.B., "Effects of Various Inhibitors on Hydrogen-Air Flame Speeds," *Combustion and Flame*, 7, pp.137-142, 1963.
4. McHale, E.T., "Survey of Vapor Phase Chemical Agents for Combustion Suppression," *Fire Res. Abstr.*, 11, No. 2, pp. 90-104, 1969.
5. Friedman, R., "Survey of Chemical Inhibition in Flames," *Fire Res. Abstr.*, 3, pp. 128-132, 1961.
6. Ibiricu, M.M., and Gaydon, A.G., "Spectroscopic Studies of the Effect of Inhibitors on Counterflow Diffusion Flames," *Combustion and Flame*, 8, pp. 51-62, 1962.
7. Babushok, V., Tsang, W., "Influence of phosphorus-containing fire suppressants on flame propagation," *Proc. of the Third Int .Conf. on Fire Res. and Eng.*, Chicago, pp. 257-267, 1999.
8. Kashiwagi, T., Gilman, J.W., McGrath, J.E., and Wann, I.-Y., "Flammability Properties of Phosphine Oxide Copolymers and of Commodity Polymers with New Flame Retardant Additives," *FRCA Fall Meeting*, Naples, FL, 1996.
9. MacDonald, M.A., Jayaweera, T.M., Fisher, E.M., and Gouldin, F.C., "Inhibition of Nonpremixed Flames by Phosphorus-Containing Compounds," *Combustion and Flame*, 116, pp. 166-176, 1999.
10. MacDonald, M.A., Jayaweera, T.M., Fisher, E.M., and Gouldin, F.C., "Variation of Chemically Active and Inert Flame-Suppression Effectiveness with Stoichiometric Mixture Fraction," *Proc. of the 27th Symp. (International) on Combust.*, pp. 2749-2756, 1998.

11. Riches, J., Grant, K., and Knutsen, L., "Laboratory Testing of Some Phosphorus-containing Compounds as Flame Suppressants," *Proceedings*, Halon Options Technical Working Conference, Albuquerque, NM, pp. 444-452, 1999.

12. Korobeinichev, O., Bolshova, T., Shvartsberg, V., Chernov, A., and Mokrushin, V., "Inhibition Effect of TMP on $CH_4/O_2/Ar$ and $H_2/O_2/Ar$ Flames," *Proceedings*, Halon Options Technical Working Conference, Albuquerque, NM, pp. 488-498, 1999.

13. Hastie, J.W., and Bonnell, D.W., *Molecular Chemistry Inhibited Combustion Systems*, National Bureau of Standards, NBSIR 80-2169, PB-81-170375, 1980.

14. Marowlewski, T.A., and Weil, E.D., "A Review of Phosphate Ester Fire Resistance Mechanisms and Their Relevance to Fluid Testing," *Fire Resistance of Industrial Fluids*, Vol. ASTM STP1284, Philadelphia, 1996.

15. Kaizerman, J.A., and Tapscott, R.E., *Advanced Streaming Agent Development. Vol. II, Phosphorus Compounds*, NMERI 96/5/32540, Wright Laboratory and Applied Research Associates, Tyndall AFB, FL, June 1996.

16. Skaggs, R.R., Daniel, R.G., Miziolek, A.W., and McNesby, K.L., "Spectroscopic Studies of Inhibited Opposed-Flow Propane-Air Flames," *Proceedings*, Halon Options Technical Working Conference, Albuquerque, NM, pp. 117-131, 1999.

17. *4th Meeting of the Parties to the Montreal Protocol on Substances that Deplete the Ozone Layer*, Copenhagen, Doc. No. UNEP/Ozl.Pro.4/15 (Nairobi: UNEP), 1992.

18. Twarowski, A., "The Effect of Phosphorus Chemistry on Recombination Losses in a Supersonic Nozzle," *Combustion and Flame*, 102, pp. 55-63, 1995.

19. Twarowski, A., "Reduction of a Phosphorus Oxide and Acid Reaction Set," *Combust. and Flame*, 102, pp. 41-54, 1995.

20. Hamins, A., Gmurczyk, G.W., Grosshandler, W.L., Rehwoldt, R.G., Vazquez, I., Cleary, T.G., Presser, C., and Seshadri, K., "Flame Suppression Effectiveness," *Evaluation of Alternative In-Flight Fire Suppressants for Full-Scale Testing in Simulated Aircraft Engine Nacelles and Dry Bays*, Section 4, NIST SP861, pp. 345-465, 1994.

21. Werner, J.H., Cool, T.A., "A Kinetic Model for the Decomposition of DMMP in a Hydrogen/Oxygen Flame," *Combustion and and Flame*, 117, pp. 78-98, 1999.

22. Luque, J., and Crosley, D. R., "LIFBASE: Database and Simulation Program (v 1.6)," SRI International Report MP 99-009, 1999.

23. Kee, R.J., Rupley, F.M., Miller, J.A., Coltrin, M.E., Grcar, J.F., Meeks, E., Moffat, H.K., Lutz, A.E., Dixon-Lewis, G., Smooke, M.D., Warnatz, J., Evans, G.H., Larson, R.S., Mitchell, R.E., Petzold, L.R., Reynolds, W.C., Caracotsios, M., W.E. Stewart, and Glarborg. P., *Chemkin Collection*, Release 3.5, Reaction Design, Inc., San Diego, CA, 1999.

24. Nishioka M., Law, C. K., and Takeno, T., "A Flame-Controlling Continuation Method for Generating S-Curve Responses with Detailed Chemistry," *Combustion and Flame*, 104, No. 3, pp. 328-342, 1996.

APPENDIX A. KINETIC MODEL FOR FLAME INHIBITION BY DMMP

	Reactions	A(f(cm,s,mol))	n	E(cal)	Ref.
1.	DMMP=PHCH3OCH3O+CH2O	3.6E12	0.	87300.	21
2.	DMMP=PCH3OCH3(OCH2)O+H	1.E14	0.	97000.	23
3.	PCH3OCH3(OCH2)O=CH3P(OCH3)O+CH2O	3.7E14	0.	38950.	21
4.	PCH3OCH3(OCH2)O=CH2O+OPCH3OCH3	1.E+14	0.	40000.	23
5.	PCH3(OCH3)2OH=POHCH3OCH3O+CH3	1.E13	0.	3000.	21
6.	POHCH3OCH3O=CH3OPO2+CH4	1.7E+12	0.	39000.	23
7.	POHCH3OCH3O=CH3PO2+CH3OH	1.7E12	0.	39000.	21
8.	P(OH)2O=H2O+PO2	1.7E+12	0.	39000.	23
9.	CH3OPO2=HOPO+CH2O	1.E+12	0.	40000.	21
10.	CH3OPO=CH3PO2	2.E11	0.	27000.	23
11.	POH(OCH3)2O=CH3OPO2+CH3OH	1.7E+12	0.	39000.	21
12.	OPCH3OCH3=CH3+CH3PO2	1.0E+14	0.	18000.	21
13.	OPCH3OCH3=CH3OPO+CH3	0.1E13	0.	30800.	23
14.	CH3P(OCH3)O=CH3PO2+CH3	1.E14	0.	18000.	21
15.	OPOHCH3+M=HOPO+CH3+M	1.0E+11	0.	30000.	23
16.	OP(OH)2OCH3=HOPO2+CH3OH	1.7E12	0.	39000.	23
17.	OPOHCH3=HOPO+CH3	1.E11	0.	20000.	21
18.	DMMP+H=PCH3OCH3(OCH2)O+H2	1.0E12	0.	4000.	21
19.	POH(OCH3)2O+H=OP(OH)2OCH3+CH3	1.0E12	0.	8000.	23
20.	OP(OH)2OCH3+H=OP(OH)3+CH3	1.0E12	0.	4000.	22
21.	P(OH)2O + H=HOPO+H2O	1.E12	0.	3000.	23
22.	PCH3OCH3(OCH2)O+H=CH2O+PHCH3OCH3O	1.0E+14	0.	0.	21
23.	PHCH3OCH3O+H=CH3P(OCH3)O+H2	1.E13	0.	8000.	23
24.	DMMP+H=POHCH3OCH3O+CH3	3.0E+12	0.	4000.	21
26.	DMMP+H=PCH3(OCH3)2OH	1.E13	0.	8000	21
27.	POHCH3OCH3O+H=OP(OH)2CH3+CH3	3.0E+12	0.	4000.	23
28.	OP(OH)3+H=P(OH)2O+H2O	3.0E+12	0.	18000.	21
29.	CH3PO2+H=HOPO+CH3	3.0e+12	0.	8000.	21
30.	CH3PO2+H=OPOHCH3	2.0E+11	0.	8000.	21
31.	CH3OPO2+H=HOPO+CH3O	1.0E+12	0.	4000.	23
32.	CH3OPO2+H=CH3PO2+OH	1.0E+12	0.	12000.	23
33.	CH3OPO2+H=HOPO2+CH3	3.0E+12	0.	10000.	23
34.	PHCH3OCH3O+H=OPCH3OCH3+H2	1.0E+14	0.	4000.	21
35.	CH3P(OCH3)O+H(+M)=PHCH3OCH3O	1.E14	0.	0.	21,mod
	LOW /	2.E20	0.0	0. /	
36.	CH3OPO+H=OPOHCH3	2.E+11	0.	8000.	23
37.	OPOHCH3+H=CH3POHOH	1.0E+14	0.	4000.	23
38.	CH3POHOH+H=OPOHCH3+H2	1.E12	0.	0.	23
39.	H+PO2+M=HOPO+M	5.E24	-2.04	645.	23
40.	H+PO+M=HPO+M	1.81E+22	-1.95	1330.	21,19
41.	H+HPO+M=HPOH+M	5.2E30	-4.28	4320.	19,fit
42.	H+HOPO=H2+PO2	3.16E+13	0.	8000.	23
43.	H+HOPO=H2O+PO	3.16E+13	0.	11930.	19,21
44.	H+P(OH)2O=H2+HOPO2	1.E13	0.	0.	23
45.	H+HOPO2=H2O+PO2	3.16E+13	0.	8000.	23
46.	HOPO2+H+M=P(OH)2O+M	9.73E+23	-2.04	10645.	23
47.	H+HPO=H2+PO	3.16E+13	0.	2500.	23
48.	H+PH=H2+P	3.16E+13	0.	5000.	19
49.	H+P+M=PH+M	6.4E20	-1.77	1790.	19,fit
50.	H+PO3=O+HOPO	3.16E+11	0.	12000.	23
51.	H+PO3=OH+PO2	3.16E+13	0.	9000.	23
52.	H+PO3+M=HOPO2+M	1.2E29	-3.66	3620.	19,fit
53.	H+H2POH=H2+HPOH	3.16E+13	0.	4150.	19
54.	H+HPOH=H2O+PH	3.16E+13	0.	4000.	23
55.	H+HPOH=H2+HPO	3.16E+13	0.	2000.	23
56.	H+HPOH+M=H2POH+M	4.6E36	-5.86	6090.	19,fit
57.	DMMP+OH=PCH3OCH3(OCH2)O+H2O	1.E12	0.	4000.	21
58.	DMMP+OH=POHCH3OCH3O+CH3O	1.E13	0.	4000.	21
59.	DMMP+OH=POH(OCH3)2O+CH3	1.E13	0.	4000.	21
60.	POH(OCH3)2O+OH=OP(OH)2OCH3+CH3O	1.E13	0.	15000.	23
61.	P(OH)2O+OH=HOPO2+H2O	3.16E12	0.	0.	22
62.	P(OH)2O+OH+M=OP(OH)3+M	1.6E23	-2.28	285.	23
63.	PCH3OCH3(OCH2)O+OH=CH2O+POHCH3OCH3O	1.0E+13	0.	0.	21
64.	POHCH3OCH3O+OH=OP(OH)2CH3+CH3O	1.0E13	0.	4000.	23
65.	OP(OH)2CH3+OH=OP(OH)3+CH3	3.E+12	0.	4000.	23
66.	PHCH3OCH3O+OH=OPCH3OCH3+H2O	3.E+13	0.	0.	21
67.	PHCH3OCH3O+OH=CH3P(OCH3)O+H2O	3.E13	0.	0.	21,mod
68.	CH3OPO2+OH=HOPO2+CH3O	3.0E+12	0.	4000.	21
69.	CH3PO2+OH=HOPO2+CH3	3.0E+12	0.	8000.	21
70.	OH+PO2+M=HOPO2+M	1.6E+24	-2.28	285.	21,19
71.	OH+PO+M=HOPO+M	1.19E+20	-1.80	1390.	21,19
72.	OH+HOPO=H2O+PO2	3.E+12	0.	0.	23
73.	OH+PO=H+PO2	3.16E+11	0.	5970.	19
74.	OH+P=H+PO	3.16E+13	0.	4650.	19

75. OH+HOPO=H+HOPO2	3.16E+11	0.	9700.	19
76. OH+PO3=O+HOPO2	3.16E+11	0.	6000.	23
77. OH+HPO=H2O+PO	3.E+12	0.	0.	23
78. OH+HPO=H+HOPO	3.16E+11	0.	12000.	19
79. OH+PH=H2O+P	3.16E+11	0.	2430.	19
80. OH+PH=H+HPO	3.16E+11	0.	4545.	19
81. OH+H2POH=H2O+HPOH	3.16E+11	0.	1600.	19
82. OH+HPOH=H2O+HPO	3.16E+11	0.	3280.	19
83. OH+PH+M=HPOH+M	7.7E17	-1.51	1530.	19,fit
84. DMMP+O=PCH3OCH3(OCH2)O+OH	5.E12	0.	8000.	23
85. O+OPOHCH3=OH+CH3PO2	3.E12	0.	0.	23
86. O+CH3PO2+M=CH3OPO2+M	1.E13	0.	0.	23
87. O+CH3PO2=CH3+PO3	3.E12	0.	6000.	23
88. O+CH3PO2=CH2O+HOPO	2.E12	0.	0.	23
89. O+P(OH)2O=HOPO2+OH	1.E13	0.	0.	23
90. O+OPOHCH3=CH3+HOPO2	3.E12	0.	5000.	23
91. O+CH3OPO=CH2O+HOPO	1.E12	0.	0.	23
92. O+CH3OPO2=HOPO2+CH2O	1.E12	0.	0.	23
93. O+PO+M=PO2+M	4.9E29	-3.95	3980.	19,fit
94. O+HOPO+M=HOPO2+M	4.8E31	-4.34	4400.	19,fit
95. O+HOPO2=O2+HOPO	1.E13	0.	10000.	23
96. O+HOPO=OH+PO2	3.16E+13	0.	0.	19
97. O+HPO=OH+PO	3.16E+13	0.	0.	23
98. O+HPO=H+PO2	3.16E+13	0.	12000.	19
99. O+PO3=O2+PO2	3.16E+13	0.	0.	19
100.O+PH=PO+H	3.16E+13	0.	2387.	19
101.O+PH=OH+P	3.16E+13	0.	3720.	19
102.O+H2POH=OH+HPOH	3.16E+13	0.	2800.	19
103.O+HPOH=H+HOPO	3.16E+13	0.	0.	19
104.O+PO2+M=PO3+M	6.E33	-5.12	5190.	19,fit
105.O+P+M=PO+M	1.5E23	-2.28	2330.	19,fit
106.O + PH + M = HPO + M	7.4E14	-0.414	420.	19,fit
107.O+HPOH=OH+HPO	3.16E+13	0.	4600.	19
108.HO2+PO2=O2+HOPO	3.16E+11	0.	630.	19
109.HO2+PO2=O+HOPO2	3.16E+11	0.	0.	19
110.HO2+PO2=OH+PO3	3.16E+11	0.	2500.	23
111.HO2+PO=O2+HPO	3.16E+11	0.	6750.	19
112.HO2+PO=O+HOPO	3.16E+11	0.	0.	19
113.HO2+PO=OH+PO2	3.16E+11	0.	1800.	19
114.HO2+HOPO=OH+HOPO2	3.16E+11	0.	3700.	19
115.HO2+PO3=O2+HOPO2	3.16E+11	0.	0.	19
116.HO2+HPO=O2+HPOH	3.16E+11	0.	10200.	19
117.HO2+P=O2+PH	3.16E+13	0.	6800.	19
118.HO2+P=OH+PO	3.16E+11	0.	1830.	19
119.HO2+PH=OH+HPO	3.16E+11	0.	1580.	19
120.HO2+PH=HPOH+O	3.16E+11	0.	0.	19
121.HO2+HPOH=O2+H2POH	3.16E+11	0.	5280.	19
122.DMMP+CH3=PCH3OCH3(OCH2)O+CH4	5.E12	0.	10000.	23
123.CH3+PO2=CH3PO2	1.E12	0.	0.	23
124.CH3+PO3+M=CH3OPO2+M	1.E16	0.	0.	23
125.CH3+PO3=PO2+CH3O	1.E13	0.	12000.	23
126.CH3+HPO=CH4+PO	1.E13	0.	4000.	23
127.CH3+HOPO=PO2+CH4	3.E12	0.	8000.	23
128.CH3+HOPO2=PO3+CH4	3.E12	0.	20000.	23
129.PO2+P=PO+PO	3.16E+13	0.	4910.	19
130.O2+P=O+PO	3.16E+13	0.	4200.	19
131.HOPO2+P=PO+HOPO	3.16E+13	0.	6850.	19
132.P + PO3 = PO + PO2	3.16E13	0.	40.	19
133.P + HPO = PO + PH	3.16E13	0.	6900.	19
136.P + HPOH = HPO + PH	3.16E13	0.	9700.	19
137.O2+PH=O+HPO	3.16E+11	0.	5723.	19
138.PH + PO2 = PO + HPO	3.16E11	0.	4800.	19
139.PH + PO2 = HOPO + P	3.16E11	0.	70.	19
140.PH + HOPO2 = HOPO + HPO	3.16E11	0.	6700.	19
141.PH + PO3 = PO2 + HPO	3.16E11	0.	0.	19
142.PH + PO3 = HOPO2 + P	3.16E11	0.	0.	19
143.PH + HPOH = P + H2POH	3.16E11	0.	6900.	19
144.PO+HOPO2=PO2+HOPO	3.16E+11	0.	9730.	19
145.O2+PO=O+PO2	3.16E+11	0.	10000.	23
146.PO+HPOH=HOPO+PH	3.16E+11	0.	0.	19
147.PO + HPOH = HPO + HPO	3.16E11	0.	10100.	19
148.PO + PO3 = PO2 + PO2	3.16E11	0.	0.	19
149.PO + O2 +M = PO3 +M	1.E15	0.	0.	23
150.PO+CH3O=CH3+PO2	1.E13	0.	3000.	23
151.PO2 + HPO = PO + HOPO	3.16E11	0.	0.	19
152.PO2 + H2POH = HOPO + HPOH	3.16E11	0.	0.	19
153.PO2 + HPOH = HOPO + HPO	3.16E11	0.	1800.	19
154.PO2 + HPOH = HOPO2 + PH	3.16E11	0.	0.	19
155.PO2+H2O2=HOPO2+OH	3.E12	0.	10000.	23
156.PO2+CH3O=HOPO+CH2O	1.E12	0.	0.	23

157.OH+HOPO2=H2O+PO3	2.E12	0.	9000.	23
158.H+HOPO2=H2+PO3	3.E12	0.	18000.	23
159.PO3 + HOPO = PO2 + HOPO2	3.16E11	0.	1450.	19
160.PO3 + HPO = PO + HOPO2	3.16E11	0.	0.	19
161.PO3 + H2POH = HOPO2 + HPOH	3.16E11	0.	0.	19
162.PO3 + HPOH = HOPO2 + HPO	3.16E11	0.	0.	19
163.PO3+CH3O=HOPO2+CH2O	1.E12	0.	0.	23
164.PO3+C2H6=HOPO2+C2H5	5.E12	0.	8000.	23
165.PO3+HCO=HOPO2+CO	1.E13	0.	0.	23
166.HPO + HPOH = PO +H2POH	3.16E11	0.	4950.	19
167.HPO+C2H5=C2H6+PO	1.E13	0.	5000.	23
168.HOPO+C2H5=C2H6+PO2	5.E12	0.	9000.	23
169.HPOH + HPOH = HPO + H2POH	3.16E11	0.	7700.	19